



Multiwavelets domain singular value features for image texture classification

RAMAKRISHNAN S., SELVAN S.

(Department of Information Technology, PSG College of Technology, Coimbatore 641 004, India)

E-mail: ram_f77@yahoo.com; drselvan@ieee.org

Received Aug. 15, 2006; revision accepted Jan. 5, 2007

Abstract: A new approach based on multiwavelets transformation and singular value decomposition (SVD) is proposed for the classification of image textures. Lower singular values are truncated based on its energy distribution to classify the textures in the presence of additive white Gaussian noise (AWGN). The proposed approach extracts features such as energy, entropy, local homogeneity and max-min ratio from the selected singular values of multiwavelets transformation coefficients of image textures. The classification was carried out using probabilistic neural network (PNN). Performance of the proposed approach was compared with conventional wavelet domain gray level co-occurrence matrix (GLCM) based features, discrete multiwavelets transformation energy based approach, and HMM based approach. Experimental results showed the superiority of the proposed algorithms when compared with existing algorithms.

Key words: Image texture classification, Multiwavelets transformation, Probabilistic neural network (PNN)

doi:10.1631/jzus.2007.A0538

Document code: A

CLC number: TP391

INTRODUCTION

The past few decades have witnessed a substantial interest in the classification of textured images, which found applications in numerous areas such as remote sensing, robot vision, crop classification, automatic tissue recognition in medical imaging and content based access to image databases.

The method chosen for feature extraction is clearly critical to the success of the texture classification. Several approaches for extraction of texture features have been proposed in literature. Most of them are based on signal processing and model-based techniques. Signal processing techniques are mainly based on texture filtering followed by energy evaluation. Varieties of model and feature based approaches using wavelet transformation has been proposed for image texture classification (Unser and Eden, 1989; Bovik *et al.*, 1990; Chang and Kuo, 1993; Laine and Fan, 1993; Teuner *et al.*, 1995; Unser, 1995; Aujol *et al.*, 2003).

Until recently, only scalar wavelets (wavelets generated by one scaling function) were widely used. But one can imagine a situation when there is more than one scaling function, for example, image classification, compression and denoising. This leads to the notion of multiwavelets, which is a more recent generalization with higher numbers of distinct scaling functions than wavelets, offering further theoretical and experimental advantages. For example, multiwavelets have been constructed that simultaneously possess symmetry, orthogonality, and compact support (Cotronei *et al.*, 1998; 2000; Tham *et al.*, 2000; Strela *et al.*, 1999; Bao and Xia, 2000; Wang, 2002; Jafari-Khouzani and Soltanian-Zadeh, 2003; Hsung *et al.*, 2005). They combine characteristics that cannot be simultaneously obtained with a single wavelet. Multiwavelets can simultaneously provide perfect reconstruction, while preserving length (orthogonality), good performance at the boundaries (via linear-phase symmetry), and a high order of approximation (vanishing moments). These features of mul-

tiwavelets are responsible for the better performance of multiwavelets over scalar wavelets in image processing applications. Specific applications where multiwavelets have been found to offer superior performance over single wavelets include signal/image classification (Wang, 2002; Jafari-Khouzani and Soltanian-Zadeh, 2003; Li and Wang, 2003), compression (Cotronei et al., 2000; Bao and Xia, 2000) and denoising (Hsung et al., 2005).

Even though many of the classification methods provide good classification performances, they have high misclassification rate when the textures are contaminated with additive white Gaussian noise (AWGN). In this paper, a novel approach using singular value decomposition (SVD) and multiwavelets transformation is presented for the classification of image textures in the presence of Gaussian noise.

Probabilistic neural networks (PNNs) that incorporate the Bayesian decision role and statistical models have been widely used for pattern classification (Specht, 1990; Raghu and Yegnanarayana, 1998). In this paper the classification of image textures is carried out using PNN.

The proposed approach defined herein is novel in the following respects:

- (1) Use of SVD on multiwavelets transformation coefficients to extract features for the texture classification.
- (2) New procedure is introduced for classifying textures in the presence of noise.
- (3) A new procedure is introduced for the selection of subbands of multiwavelets transformation.

This paper is organized as follows. Section 2 briefly introduces multiwavelets transformation. Proposed multiwavelets domain singular value based features for image texture classification are presented in Section 3. The details of the PNN architecture and method used for finding the smoothing parameter are provided in Section 4. Experimental results and discussions are provided in Section 5. Conclusions are drawn in Section 6.

MULTIWAVELETS TRANSFORMATION

In multiresolution analysis of multiplicity r , the multiscaling functions and the corresponding multiwavelets are usually written as vectors $\varphi(t)$ and $\psi(t)$, respectively, satisfying the matrix dilation equation:

$$\varphi(t) = \sqrt{2} \sum_{k=-\infty}^{\infty} H_k \varphi(2t - k), \tag{1}$$

and matrix wavelet equation

$$\psi(t) = \sqrt{2} \sum_{k=-\infty}^{\infty} G_k \psi(2t - k), \tag{2}$$

where H_k and G_k are lowpass and highpass filter coefficients respectively.

Unlike scalar wavelet in which Mallat's pyramid algorithms can be employed directly, the application of multiwavelets requires the input signal to be first vectorized (which is a problem popularly known as multiwavelets pre-filtering). To address this problem, many approaches have been proposed in (Hardin and Roach, 1998; Xia, 1998; Bao and Xia, 2000; Johnson, 2000; Strela et al., 1999; Attakitmongcol et al., 2001; Hsung et al., 2003). Decomposition of the multiwavelets transformation for 2D images was carried out using tensor products of the 1D filter banks as illustrated in Fig.1.

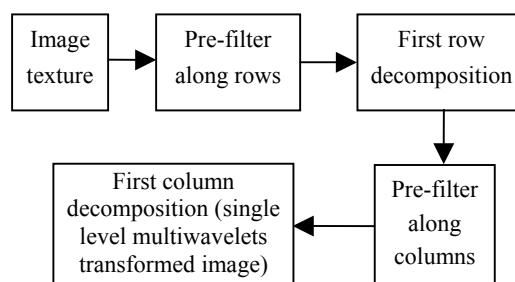


Fig.1 Single level decomposition of the multiwavelets transformation

Result after single level decomposition of the multiwavelets transformation has 16 subbands as illustrated below

L1L1	L2L1	H1L1	H2L1
L1L2	L2L2	H1L2	H2L2
L1H1	L2H1	H1H1	H2H1
L1H2	L2H2	H1H2	H2H2

Here a typical block H2L1 contains low-pass coefficients corresponding to the first scaling function in the horizontal direction and high-pass coefficients corresponding to the second wavelet in the vertical direction. Various multiwavelets used in the proposed approach are listed in Table 1 along with their properties and the corresponding pre-filter coefficients are listed in Table 2.

Table 1 Multiwavelets used in the proposed approach

	Multiwavelets			
	SA4	CL	Cardbal4	GHM
Reference	(Tham <i>et al.</i> , 2000)	(Chui and Lian, 1996)	(Selesnick, 2000)	(Donovan <i>et al.</i> , 1996)
Orthogonal or not	Yes	Yes	Yes	Yes
Symmetric or not	Yes	Yes	Yes	Yes
No. of scaling functions	2	2	2	2
No. of scaling coefficients	4	3	12	4
No. of wavelet coefficients	4	3	12	4
Approximation order	1	2	4	2

Table 2 Corresponding pre-filters used in constructing multiwavelets transformation

	Multiwavelets			
	SA4	CL	Cardbal4	GHM
Pre-filter matrix*	$\begin{bmatrix} 0.7071 & 0.7071 \\ -0.7071 & 0.7071 \end{bmatrix}$	$\begin{bmatrix} 0.2500 & 0.2500 \\ 0.2743 & -0.2743 \end{bmatrix}$	As it is balanced, no pre-filter is needed	$\begin{bmatrix} 0.11942337067748 & -0.00598315472909 \\ 0.99158171438258 & -0.04967860804828 \\ 0.04967860804828 & 0.99158171438250 \\ -0.00598315472909 & -0.11942337067748 \end{bmatrix}^T$

* Size: 'r' by 'r×l' real array. 'r' is the number of scaling functions, 'l' is the number of coefficients in the pre-filter. The matrix is organized as: $PR=[P_1 P_2 \dots P_l]$

PROPOSED APPROACH

Conventional multiwavelets transformation produces 16 subbands in the first level and 28 subbands in the second level decomposition; in general it provides '4+12L' subbands for L decomposition levels. Unlike conventional multiwavelets transformations, which considers all the four low pass subbands (L1L1, L1L2, L2L1 and L2L2) of the first level decomposition for performing the second level of decomposition, the proposed approach selects one of four low pass subbands from the first level based on the discrimination ability (details are provided in the next subsection). All the 16 subbands from the first level and 16 subbands from the second level corresponding to a selected subband from the first level were considered for further processing. Proposed approach consists of training and testing phases. During both phases feature vectors are formed using the procedure given below.

SVD was applied on all the 32 subband coefficient matrices after introducing non-linearity. Lower singular values were truncated to achieve better classification rate under noisy environment. The remaining singular values were used to extract features for image texture classification.

During training phase, feature vectors of the known classes were extracted and used to train the PNN. During the testing phase, the feature vector of the image to be classified was presented to the PNN and PNN classified the texture based on Bayes's decision rule. Proposed approach is illustrated in Fig.2.

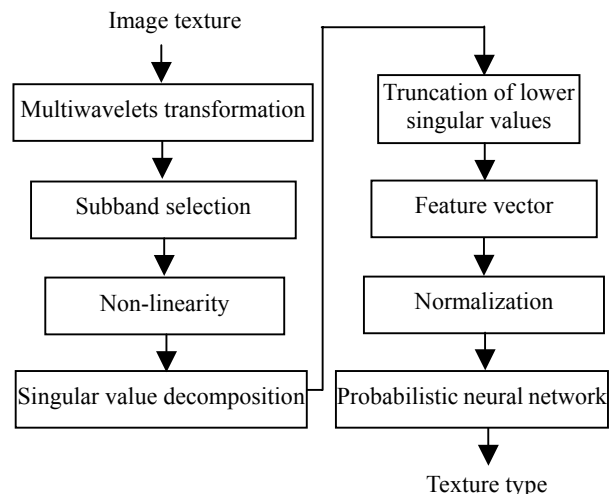


Fig.2 Block diagram of the proposed approach

Subband selection

Conventional wavelet transformation has single

low pass region at each level and further decomposition is only carried out subsequently in the low pass region. However in multiwavelets transformation we have four low pass regions, hence our task is to select the best one out of these four regions for performing the next level decomposition. This is achieved by using ‘ P_i ’, the ratio between the arithmetic and geometric mean of the variances at all the 16 subbands at the second level corresponding to each low pass subband at the first level ($i=1$ for L1L1, 2 for L1L2, 3 for L2L1 and 4 for L2L2).

Let σ_k^2 denote the variance of the output of the k th subband, and $k=1, \dots, M$ (Here $M=16$). Let

$$P_i = \frac{1}{M} \sum_{k=1}^M \sigma_k^2 / \left(\prod_{k=1}^M \sigma_k^2 \right)^{\frac{1}{M}}, \quad (3)$$

P_i is generally greater than 1 and equal to 1 if all the variances are equal. When all the variances are equal, it is not possible to clearly distinguish between smooth and detailed components of multiwavelets transformation coefficients. Hence further processing of those subbands is not helpful for the classification. One of the low pass subbands of the first level which has the highest P_i value was selected and the corresponding 16 subbands at the second level were considered for further processing. Hereafter all the processing was carried out using 32 subbands, i.e., on all the 16 subbands from the first level and selected 16 subbands from the second level. This means that the features of two different textures might have been calculated from different subbands. However, different subbands were used to extract the texture features and they were compared for performing the classification in (Chang and Kuo, 1993), it is expected that the decomposition tree will be the same for the texture samples belonging to the same texture.

Introducing non-linearity

Non-linearity is introduced on subband coefficient matrices to make them less sensitive to local variations (Unser and Eden, 1989; Unser, 1995). Numerous nonlinearities such as magnitude, squaring and rectified sigmoid have been applied in the literature. Unser (1995) proposed and tested several nonlinearities and concluded that squaring non-line-

arity is the best amongst others. Even though these non-linearities are most suited for texture segmentation, they were suggested for texture classification (Randen and Husoy, 1999). In this paper we propose a modified squaring non-linearity employed in a 3×3 neighborhood, the details of which are given below.

Total energy at each subband is calculated for multiwavelets transformation coefficients using the following formula

$$W_i = \frac{1}{MN} \sum_{j=1}^M \sum_{k=1}^N |x_i(j, k)|^2. \quad (4)$$

W_i is overall energy in the i th subband, $X_i(j, k)$ multiwavelets transformation coefficients at location (j, k) in the i th subband. Then at each location (j, k) the local energy is computed in a 3×3 neighborhood using the formula

$$L_i(j, k) = \frac{1}{9} \sum_{m=0}^2 \sum_{n=0}^2 |x_i(j-1+m, k-1+n)|^2. \quad (5)$$

The local energies $L_i(j, k)$ are normalized using

$$a_i(j, k) = L_i(j, k) / W_i. \quad (6)$$

Singular value decomposition

SVD is a very powerful tool and mainly used for dimensionality reduction, solving system of linear equations and noise reduction. In this paper we use SVD for extracting features for image textures and reducing the effect of AWGN.

Let A_i be the i th multiwavelets transformation coefficient subband matrix after introducing the non-linearity. SVD is then applied on matrices A_i of size $M \times N$ such that

$$A_i = U_i \Sigma_i V_i^T, \quad (7)$$

here U_i are orthogonal $M \times M$ matrices whose columns are the eigenvectors of $A_i A_i^T$, V_i are $N \times M$ matrices whose columns are eigenvectors of $A_i^T A_i$, and Σ_i are $M \times M$ diagonal matrices with nonnegative diagonal elements in decreasing order whose entries (the “singular values”) are the square roots of the corresponding eigenvalues of $A_i A_i^T$.

Truncation of lower singular values

In order to achieve better classification rate under noisy environment, lower singular values are truncated. The number of singular values included in approximation was chosen by considering the ratio of the energy associated with the first singular value to the total energy. The first k singular values out of M singular values are selected for further processing, k is obtained using

$$k = Ms_1^2 / \sum_{i=1}^M s_i^2, \quad (8)$$

where s_i denotes the i th singular value, $i=1, 2, \dots, M$.

Our assumption on truncating the lower singular values for classifying the textures in the presence of AWGN is validated using a metric, Impact Factor (IF), which is defined below

$$IF(i) = |SV_{\text{Original image}}(i) - SV_{\text{Noisy image}}(i)| / SV_{\text{Original image}}(i). \quad (9)$$

IF for lower and higher singular values is shown in Fig.3 for one of the subbands for the image texture, beach sand. It can be seen from the figure that impact factor is more pronounced on lower singular values than that on higher singular values. This finding is applicable to all image textures at all subbands. Hence, the truncation of lower singular values allows us to effectively classify the textures in the presence of AWGN.

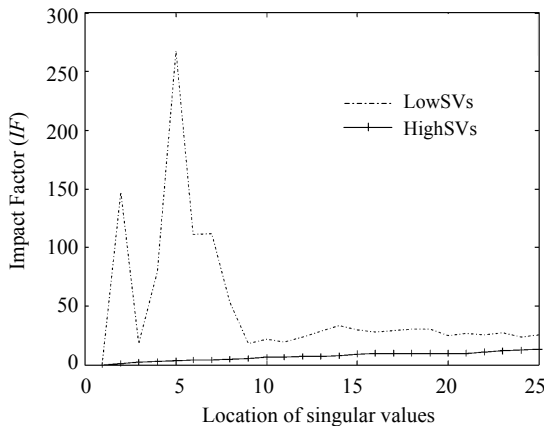


Fig.3 Impact factor to validate the truncation of lower singular values

Singular values based features

The singular values and their distribution carry

useful information about the image. For an image with random textural content, its energy will spread over all the singular values. On the other hand, for a smooth image with no texture, the first singular value will be dominant while all the others are almost zero.

In most cases, the first (largest) singular value roughly corresponds to the mean of the image, thus closely relates to the spectral features, while all the other singular values provide detailed information about the spatial content of the image which relates to the textural features (Song and Zhang, 1999; Kakarala and Ogunbona, 2001). Singular values provide the energy information of the image as well as knowledge on how the energy is distributed over the subspace. They contain the contributions from both the spectral and textural aspects of the image. Hence we used singular values for extracting features for image texture classification.

A large variety of texture features based on GLCM have been proposed (Baraldi and Parmiggiani, 1995; van de Wouwer *et al.*, 1999). In this paper we adopted features such as energy, entropy, local homogeneity from GLCM and one more new feature, max-min ratio.

Following features are extracted from the singular values.

(1) Energy

Energy shows the amount of signal in a specific resolution.

$$F_1 = \frac{1}{k} \sum_{i=1}^k s_i^2, \quad (10)$$

where F_1 denotes the energy of the singular values.

(2) Entropy

Entropy shows the non-uniformity of the singular values.

$$0 \leq F_2 = -\frac{1}{\log k} \sum_{i=1}^k p_i \log p_i \leq 1, \quad (11)$$

where F_2 denotes the entropy of the singular values. And

$$p_i = s_i^2 / \sum_{i=1}^k s_i^2. \quad (12)$$

p_i indicates the relative significance of the i th singular values in terms of the fraction of the overall expression that they capture.

F_2 measures the complexity of the image from the distribution of the overall expression between the different singular values. $F_2=0$ corresponds to an ordered and redundant image in which all expressions are captured by a single singular value and $F_2=1$ corresponds to a disordered and random image where all the singular values are equally expressed.

(3) Local homogeneity

Local homogeneity measures smoothness of an image in a local neighborhood. Here, local homogeneity measures the trends present in the singular values.

$$F_3 = \sum_{i=1}^k \frac{S_i}{1+i^2}, \quad (13)$$

where F_3 denotes the homogeneity of the singular values.

(4) Max-min ratio

Ratio between maximum and minimum singular value is used as one of the features here.

$$F_4 = S_{\max}/S_{\min}, \quad (14)$$

where F_4 denotes the ratio between maximum and minimum singular values among the selected singular values.

Both the individual features $F_1 \sim F_4$ and the combined features such as F_1+F_2 , F_1+F_3 , F_1+F_4 , F_2+F_3 , F_2+F_4 , F_3+F_4 are used for classifying image textures. The classification is carried out using PNNs.

PROBABILISTIC NEURAL NETWORK

PNN is a kind of supervised neural network that is widely used in the area of pattern recognition, nonlinear mapping, and estimation of probability of class membership and likelihood ratios. The original PNN structure by Specht (1990) is a network formulation of probability density estimation. PNN has proven to be more time efficient than conventional back-propagation based networks and has been recognized as an alternative in real-time classification problems.

The architecture of the PNN is shown in Fig.4. The PNN has three layers feed forward network including input layer, pattern layer and summation layer. The input layer unit does not perform any computation

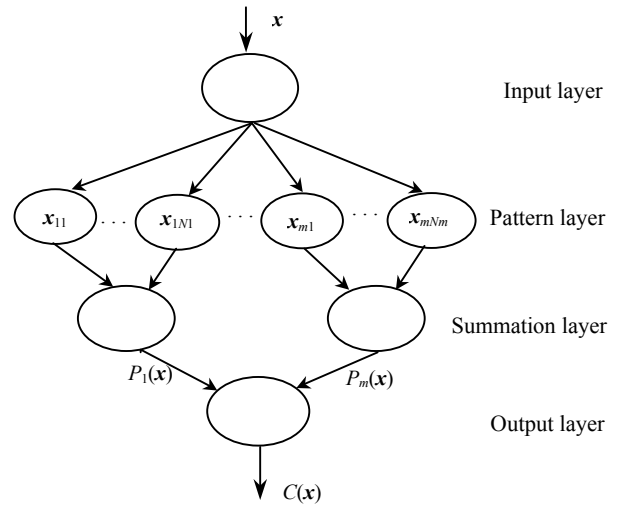


Fig.4 Architecture of the probabilistic neural network

and simply distributes the input to the neurons in the pattern layer. On receiving a pattern x from the input layer, the neuron x_{ij} of the pattern layer computes its output using

$$\phi_{ij}(x) = \frac{1}{(2\pi)^{0.5d} \sigma^d} \exp \left[-\frac{(x - x_{ij})^T (x - x_{ij})}{2\sigma^2} \right], \quad (15)$$

where d denotes the dimension of the pattern vector x , σ is the smoothing parameter and x_{ij} is the neuron vector. The smoothing parameter σ defines the width of the bell curve that surrounds each sample point.

The summation layer neurons compute the maximum likelihood of pattern x being classified into C_i by summarizing and averaging the output of all neurons that belong to the same class using

$$P_i(x) = \frac{1}{N_i (2\pi)^{0.5d} \sigma^d} \sum_{j=1}^{N_i} \exp \left[-\frac{(x - x_{ij})^T (x - x_{ij})}{2\sigma^2} \right], \quad (16)$$

where N_i denotes the total number of samples in class C_i .

If the *a priori* probabilities for each class are the same, and the losses associated with making an incorrect decision for each class are the same, the decision layer unit classifies the pattern x in accordance with the Bayes's decision rule based on the output of all the summation layer neurons using

$$\hat{C}(x) = \arg \max \{P_i(x)\}, \quad i = 1, 2, \dots, m, \quad (17)$$

where $\hat{C}(x)$ denotes the estimated class of the pattern x and m is the total number of classes in the training samples.

As we have selected 32 subbands from two levels of multiwavelets transformation, we have 32 features ($d=32$) from Brodatz texture album (Brodatz, 1966). We have created 432 subimages in our database. Out of these 432 subimages, 108 subimages are used for training and the other 324 for testing (details are presented in Section 5). For each texture we have 4 disjoint patterns for training. Hence in this work $m=27$ and $N1=N2=\dots=Nm=4$.

Proper choice of the value for σ is critical to the performance of the PNN. There is no general method available to determine σ , it is usually determined by changing its value minutely and examining the corresponding recognition accuracy. We have normalized the features before presenting them for PNN training using the following expression.

$$\hat{F}_{ij} = (F_{ij} - \mu_j) / \sigma_j, \quad (18)$$

where F_{ij} is the j th feature of the i th image, μ_j and σ_j are mean and standard deviation of feature j in the training set respectively. As the smoothing parameter σ defines the width of the bell curve that surrounds each sample point, we selected $\sigma=0.25$, which is an average value of variances of patterns presented for training.

For each pattern the smoothing parameter is allowed to vary within a given range $[0, 1]$. The average classification rate vs σ is shown in Fig.5. If σ is small (i.e., $\sigma \in [0, 0.1]$), individual training cases will be considered only in isolation and we will be left with

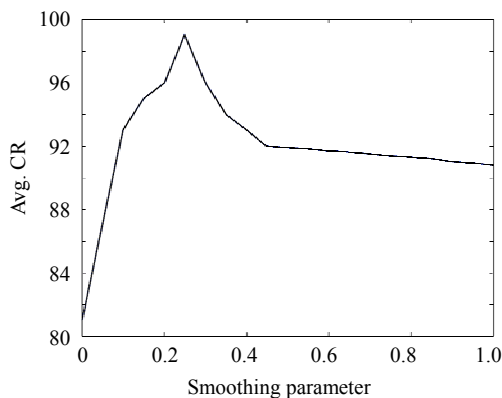


Fig.5 Average classification rate vs smoothing parameter

essentially a nearest-neighbor classifier. However, if the value of σ is high (i.e., $\sigma \in [0.5, 1]$), details of the density will be blurred together. It may be observed from the figure that the average classification rate is higher around $\sigma=0.25 \pm 0.05$.

RESULTS AND DISCUSSIONS

In order to demonstrate the effectiveness of the proposed approach various experiments were performed. Twenty-seven image textures from the Brodatz texture album (Brodatz, 1966) as listed in Table 3 (using the standard notation in this texture database) have been selected.

Table 3 List of textures selected from Brodatz texture

Texture ID					
D1	D18	D39	D53	D80	D105
D2	D19	D41	D56	D83	D111
D4	D20	D46	D57	D94	
D8	D21	D47	D77	D96	
D11	D35	D51	D78	D104	

These are 512×512 images from different natural scenes. Each of the 512×512 images is divided into sixteen 128×128 non-overlapping subimages. Hence considering 27 different textures 432 subimages are created in the database. Out of these 432 subimages, 108 subimages (four subimages per class) are used for training and the other 324 for testing. Samples of image textures used in this paper are shown in Fig.6.

Experiments were carried out to test the performance of the proposed approach with features $F_1 \sim F_4$ (individually and combination of two) using PNN. The results are presented in Table 4. From the results it is clear that the entropy feature (F_2) performs better than other individual features. Combined features F_1+F_3 , F_1+F_4 , and F_3+F_4 have improvement in classification rate compared to that of the corresponding individual features (F_1 , F_3 , and F_4). This improvement is achieved at the cost of twofold increase in terms of number of features, which is prohibitive. Combining any one of the three features with F_2 gives just one percent improvement in classification rate, which is not worth spending. Any combinations of three features (using $F_1 \sim F_4$) may not trade off well between classification rate and number of features.

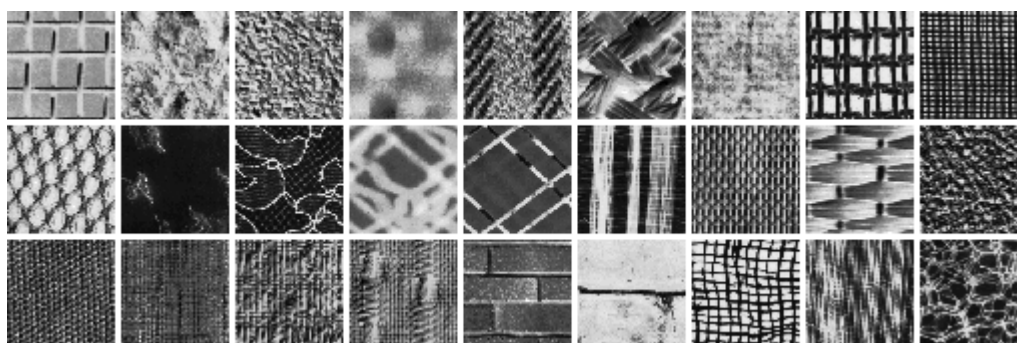


Fig.6 Image textures from Brodatz album used in this paper: from left to right and top to bottom: D1, D2, D4, D8, D11, D18, D19, D20, D21, D35, D39, D41, D46, D47, D51, D53, D56, D57, D77, D78, D80, D83, D94, D96, D104, D105 and D111

Table 4 Classification rate of the proposed approach for various categories

Image texture	Classification rate									
	F_1	F_2	F_3	F_4	F_1+F_2	F_1+F_3	F_1+F_4	F_2+F_3	F_2+F_4	F_3+F_4
D1	90	100	92	93	100	96	94	100	100	95
D2	93	98	94	91	99	96	95	100	99	96
D4	90	100	92	90	100	96	92	100	100	94
D8	94	100	96	92	100	98	96	100	100	99
D11	91	96	93	94	98	96	98	98	100	96
D18	92	98	94	90	99	98	94	99	99	98
D19	90	98	92	90	99	96	93	99	99	95
D20	90	100	94	92	100	97	94	100	100	96
D21	89	99	92	91	100	97	92	100	100	94
D35	93	98	94	93	99	98	96	100	100	96
D39	94	96	96	92	100	98	98	98	99	98
D41	91	97	94	91	98	96	94	99	98	96
D46	93	97	94	91	98	96	96	99	98	96
D47	92	96	94	90	98	97	96	98	99	98
D51	92	98	96	92	100	98	94	100	99	98
D53	91	98	94	91	100	97	96	100	100	95
D56	94	100	96	94	100	98	98	100	100	98
D57	95	99	96	91	100	98	98	100	100	98
D77	93	96	94	92	98	96	96	98	98	96
D78	94	98	96	89	100	98	96	100	99	98
D80	92	98	94	92	100	96	94	100	99	96
D83	91	97	92	94	98	96	96	99	99	96
D94	92	98	93	95	99	98	98	100	100	98
D96	91	97	94	93	99	97	96	99	99	96
D104	93	98	96	93	100	98	96	100	99	98
D105	93	98	94	92	99	97	96	100	100	96
D111	93	100	94	94	100	98	94	100	100	96
Avg. CR	92	98	94	92	99	97	95	99	99	97
κ	0.72	0.89	0.76	0.73	0.91	0.87	0.78	0.93	0.90	0.86

Classification rates are widely used as a measure to assess the performance of the classifier. It only provides the overall assessment, not providing detailed assessment. Confusion matrix (CM) is often used as a tool to visualize the performance of the classifier. Each column of the matrix represents the instances in a recognized class, while each row represents the instances in an actual class. One benefit of a CM is that it is easy to see if the classifier is confusing two classes (i.e., commonly mislabelling one as another). However, when the total number of classes handled by the classifier is large, it is not feasible to draw the CM, because the CM size is $M \times M$ if M is the total number of classes. Kappa value (also called the kappa coefficient), used as a substitute of the CM, is a measure of classification agreement, which is defined as follows:

$$\kappa = \left(N \sum_{i=1}^r X_{ii} - \sum_{i=1}^r X_{i+} X_{+i} \right) / \left(N^2 - \sum_{i=1}^r X_{i+} X_{+i} \right),$$

where r is the number of rows in the CM, X_{ii} the number of observations in row i column i , X_{i+} the marginal total of row i (to the right of the matrix), X_{+i} the marginal total of column i (to the bottom of the matrix), N the total number of samples included in the matrix.

A kappa value of 1 means a statistically perfect modeling whereas a 0 means every model value was different from the actual value. A kappa value of 0.7 or higher is generally regarded as good statistical correlation, but of course, the higher the value, the better the correlation. The kappa value is listed at the end of Table 4. It may be observed that the value is higher for individual F_2 , and any combination of two features which has F_2 as one of the components.

Ratio between average between-class-distance and average within-class-distance is used as a measure of separability of features employed. Higher value of separability ratio gives better discrimination. The ratio for both individual and combined features is listed in Table 5. Table 5 ascertains the results obtained in Table 4. From Tables 4 and 5, singular value entropy (F_2) performs better than other features. Hence in all our further studies, F_2 alone is used as the feature.

Table 5 Separability ratio for various features listed in Table 2

Features	Separability ratio
F_1	7.2
F_2	10.5
F_3	8.3
F_4	7.9
F_1+F_2	11.2
F_1+F_3	10.1
F_1+F_4	9.6
F_2+F_3	11.8
F_2+F_4	11.4
F_3+F_4	10.2

The proposed SVD based approach has been tested for noisy images. Gaussian random noise with zero mean and non-zero variance is added to image textures. The variances are determined based on the desired signal to noise ratio.

Experiments were conducted to test the performance of the proposed approach with various multiwavelets basis functions listed in Table 1. Fig.7 shows the average classification rate (Avg. CR) of the proposed approach with various multiwavelets basis at various PSNR values. It can be seen from the figure that classification rate of various basis are almost the same and hence the selection of multiwavelets basis is insignificant. We used GHM multiwavelets with corresponding prefilter listed in Table 2 for all our experiments.

Classification rate of the proposed approach at various PSNR values with multiwavelets and wavelet transformation is shown in Fig.8. Singular value

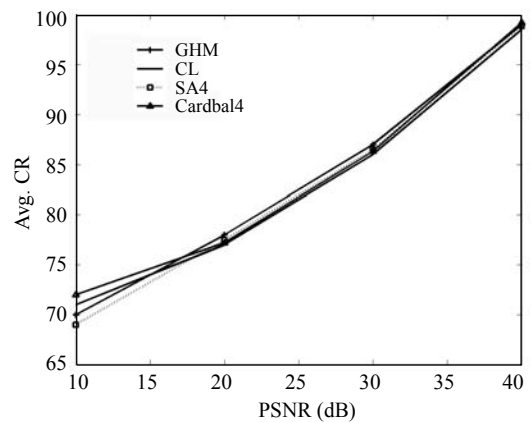


Fig.7 PSNR vs average classification rate of the proposed approach for various multiwavelets basis

entropies are used as features for both multiwavelets and wavelets transformations. We have used db6 wavelet basis function for performing the wavelet decompositions. In order to make the comparison fair with multiwavelets transformation, almost the same number of features are extracted from wavelet transformation. Unlike conventional wavelet transformation in which further decomposition is only carried out subsequently in the low pass region, here decomposition is carried out on selected subbands at each level as in (Chang and Kuo, 1993), but using the proposed metric P_i given in Eq.(4) (refer to Section 3). It can be seen from the figure that on an average, the proposed approach with multiwavelets gives approximately 5 percent improvements over the approach with wavelet.

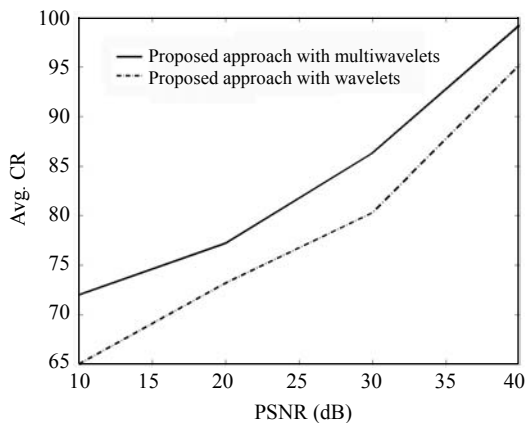


Fig.8 PSNR vs average classification rate of the proposed approach with multiwavelets and wavelet

Trade off between average classification rate and PNSR of the proposed approach with singular value entropy, wavelet domain hidden Markov model based approach (Fan and Xia, 2003), wavelet domain GLCM based approach (van de Wouwer *et al.*, 1999) and discrete multiwavelets transformation energy based approach (Li and Wang, 2003) is presented in Fig.9. It can be seen from the figure that the classification rate of the proposed approach is better than those of the other three approaches. This improvement in classification rate under noisy environment is achieved due to the truncation of the lower singular values (refer to Section 3).

Fig.10 shows the trade off between test to train sample ratio and average classification of the proposed approach with singular value entropy, wavelet domain hidden Markov model based approach

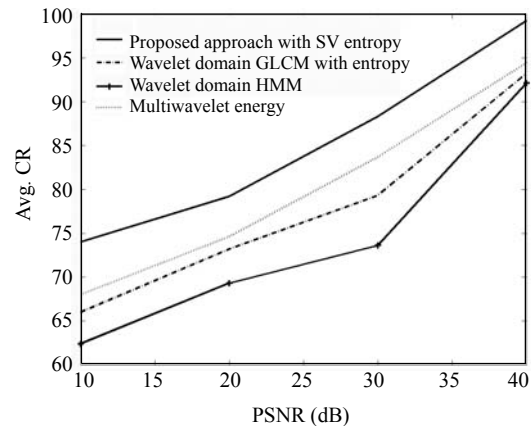


Fig.9 PSNR vs average classification rate for the proposed approach, GLCM based approach, HMM based approach and multiwavelets energy based approach

(Fan and Xia, 2003), wavelet domain GLCM based approach (van de Wouwer *et al.*, 1999) and energy of discrete multiwavelets transformation based approach (Li and Wang, 2003). It may be observed from the figure that classification rate does not change much for all the four approaches up to the test to train ratio of 0.25. However, when the number of testing sample increases, the classification rate of the HMM based approach falls more rapidly than GLCM based approach and multiwavelets energy based approach. Compared to other approaches, falling rate of the proposed approach is lower. In a test to train sample ratio of 8 (i.e. 48 samples are used for training and 384 samples are used for testing), the classification rate of the proposed, GLCM, HMM and discrete multiwavelet energy based approaches are 96, 72, 64, and 77 respectively.

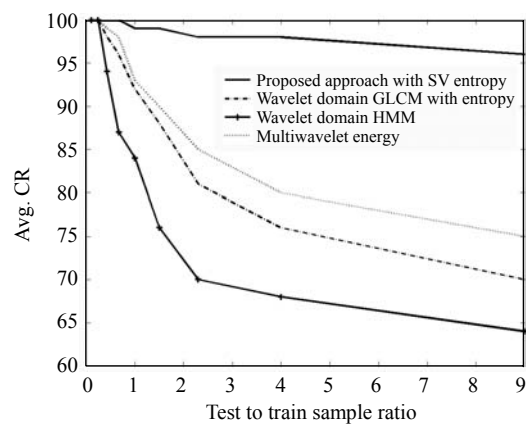


Fig.10 Average classification rate vs test to train sample ratio for the proposed approach, GLCM based approach, HMM based approach, multiwavelets energy based approach

All the experiments were performed using MATLAB on a machine with a 2 GHz Pentium IV processor. Approximately the time required for the extraction of a single feature vector is 3 s for the proposed approach, 2 s for GLCM based approach, 6 s for the wavelet domain HMM based approach and less than 2 s for multiwavelets energy based approach.

CONCLUSION

The new features based approach for image texture classification is proposed using multiwavelet domain singular values. Out of so many features suggested for GLCM, three of them namely energy, entropy and local homogeneity are considered in this work. The remaining GLCM features were also experimented on and found to be ill-suited for this setup. Singular value entropy performs better than the other individual features. Combining two or more features gives only 1%~3% improvement in classification, but the cost paid for this improvement in terms of number of features is prohibitive. Further improvement is possible with suitable feature selection methods and feature fusion methods. Classification was carried out using probabilistic neural network. Conventional PNN was adopted with fine tuning to find the smoothing factor. Future research is underway to design suitable algorithm for obtaining the parameters of PNN such as smoothing factor. Due to truncation of lower singular values, classification rate of the proposed approach is found to be better in noisy environment.

ACKNOWLEDGEMENTS

The authors would like to thank the Management and Principal, PSG College of Technology, Coimbatore for their continuous support and encouragement and, for providing the facilities required to complete this work. The authors are also grateful to the referees for their valuable suggestions in improving the technical presentation of this paper.

References

Attakitmongkol, K., Hardin, D.P., Wilkes, D.M., 2001. Multiwavelets prefilters. II. Optimal orthogonal prefilters. *IEEE Trans. Image Processing*, **10**(10):1476-1487. [doi:10.1109/83.951534]

Aujol, J., Aubert, G., Blanc-Feraud, L., 2003. Wavelet-based level set evolution for classification of textured images. *IEEE Trans. Image Processing*, **12**(12):1634-1641. [doi:10.1109/TIP.2003.819309]

Bao, K., Xia, X.G., 2000. Image compression using a new discrete multiwavelets transformation and a new embedded vector quantization. *IEEE Trans. Circuits Syst. Video Technol.*, **10**(6):833-842. [doi:10.1109/76.867920]

Baraldi, A., Parmiggiani, F., 1995. An investigation of the textural characteristics associated with gray level co-occurrence matrix statistical parameters. *IEEE Trans. Geosci. Remote Sensing*, **33**(2):293-304. [doi:10.1109/36.377929]

Bovik, A.C., Clark, M., Geisler, W.S., 1990. Multichannel texture analysis using localized spatial filters. *IEEE Trans. Pattern Anal. Machine Intell.*, **12**(1):55-73. [doi:10.1109/34.41384]

Brodatz, P., 1966. Textures: A Photographic Album for Artists and Designers. Dover, New York.

Chang, T., Kuo, C.C.J., 1993. Texture analysis and classification with tree-structured wavelet transformation. *IEEE Trans. Image Processing*, **2**(4):429-441. [doi:10.1109/83.242353]

Chui, C.K., Lian, J., 1996. A study on orthonormal multiwavelets. *Appl. Numer. Math.*, **20**(3):273-298. [doi:10.1016/0168-9274(95)00111-5]

Cotronei, M., Montefusco, L.B., Puccio, L., 1998. Multiwavelets analysis and signal processing. *IEEE Trans. Circuits Syst. II*, **45**(8):970-987. [doi:10.1109/82.718807]

Cotronei, M., Lazzaro, D., Montefusco, L.B., Puccio, L., 2000. Image compression through embedded multiwavelets transformation coding. *IEEE Trans. Image Processing*, **9**(2):184-189. [doi:10.1109/83.821728]

Donovan, G., Geronimo, J.S., Hardin, D.P., Massopust, P.R., 1996. Construction of orthogonal wavelets using fractal interpolation functions. *SIAM J. Math. Anal.*, **27**(4):1158-1192. [doi:10.1137/S0036141093256526]

Fan, G.L., Xia, X.G., 2003. Wavelet-based texture analysis and synthesis using hidden Markov models. *IEEE Trans. Circuits Syst. I: Fundam. Theory Appl.*, **50**(1):106-120. [doi:10.1109/TCSI.2002.807520]

Hardin, D.P., Roach, D.W., 1998. Multiwavelets prefilters-I: orthogonal prefilters preserving approximation order p less than 2. *IEEE Trans. Circuits Syst. II: Analog Digital Signal Processing*, **45**(8):1106-1112. [doi:10.1109/82.718820]

Hsung, T.C., Sun, M.C., Lun, D.P.K., Siu, W.C., 2003. Symmetric prefilters for multiwavelets. *IEE Proc. Vision, Image and Signal Processing*, **150**(1):59-68. [doi:10.1049/ip-vis:20030164]

Hsung, T.C., Lun, D.P.K., Ho, K.C., 2005. Optimizing the multiwavelets shrinkage denoising. *IEEE Trans. Signal Processing*, **53**(1):240-251. [doi:10.1109/TSP.2004.838927]

Jafari-Khouzani, K., Soltanian-Zadeh, H., 2003. Multiwavelets grazing of pathological images of prostate. *IEEE Trans. Biomed. Eng.*, **50**(6):697-704. [doi:10.1109/TBME.2003.812194]

- Johnson, B.R., 2000. Multiwavelets moments and projection prefilters. *IEEE Trans. Signal Processing*, **48**(11):3100-3108. [doi:10.1109/78.875467]
- Kakarala, R., Ogunbona, P.O., 2001. Signal analysis using a multiresolution form of the singular value decomposition. *IEEE Trans. Image Processing*, **10**(5):724-735. [doi:10.1109/83.918566]
- Laine, A., Fan, J., 1993. Texture classification by wavelet packet signatures. *IEEE Trans. Pattern Anal. Machine Intell.*, **15**(11):1186-1191. [doi:10.1109/34.244679]
- Li, S.T., Wang, Y.N., 2003. Texture classification using discrete multiwavelets transformation. *AMSE Periodicals*, **46**(1):1-14.
- Nguyen, T.T., Oraintara, S., 2005. Multiresolution direction filterbanks: theory, design, and applications. *IEEE Trans. Signal Processing*, **53**(10):3895-3905. [doi:10.1109/TSP.2005.855410]
- Raghu, P.P., Yegnanarayana, B., 1998. Supervised texture classification using a probabilistic neural network and constraint satisfaction model. *IEEE Trans. Neural Networks*, **9**(3):516-522. [doi:10.1109/72.668893]
- Randen, T., Husoy, J.H., 1999. Filtering for texture classification: a comparative study. *IEEE Trans. Pattern Anal. Machine Intell.*, **21**(4):291-310. [doi:10.1109/34.761261]
- Selesnick, I.W., 2000. Balanced multiwavelets bases based on symmetric FIR filters. *IEEE Trans. Signal Processing*, **48**(1):184-191. [doi:10.1109/78.815488]
- Song, L.P., Zhang, S.Y., 1999. Singular value decomposition-based reconstruction algorithm for seismic travel-time tomography. *IEEE Trans. Image Processing*, **8**(8):1152-1154. [doi:10.1109/83.777099]
- Specht, D.F., 1990. Probabilistic neural networks. *Neural Networks*, **3**(1):109-118. [doi:10.1016/0893-6080(90)90049-Q]
- Strela, V., Heller, P.N., Strang, G., Topiwala, P., Heil, C., 1999. The application of multiwavelets filterbanks to image processing. *IEEE Trans. Image Processing*, **8**(4):548-563.
- Teuner, A., Pichler, O., Hosticka, B.J., 1995. Unsupervised texture segmentation of images using tuned matched Gabor filters. *IEEE Trans. Image Processing*, **4**(6):863-870. [doi:10.1109/83.388091]
- Tham, J.Y., Shen, L., Lee, S.L., 2000. A general approach for analysis and application of discrete multiwavelets transforms. *IEEE Trans. Signal Processing*, **48**(2):457-464. [doi:10.1109/78.823972]
- Unser, M., Eden, M., 1989. Multiresolution feature extraction and selection for texture segmentation. *IEEE Trans. Pattern Anal. Machine Intell.*, **11**(7):717-728. [doi:10.1109/34.192466]
- Unser, M., 1995. Texture classification and segmentation using wavelet frames. *IEEE Trans. Image Processing*, **4**(11):1549-1560. [doi:10.1109/83.469936]
- van de Wouwer, G., Scheunders, P., van Dyck, D., 1999. Statistical texture characterization from discrete wavelet representations. *IEEE Trans. Image Processing*, **8**(4):592-598. [doi:10.1109/83.753747]
- Wang, J.W., 2002. Multiwavelet packet transforms with application to texture segmentation. *Electron. Lett.*, **38**(18):1021-1023. [doi:10.1049/el:20020723]
- Xia, X.G., 1998. A new prefilter design for discrete multiwavelets transforms. *IEEE Trans. Signal Processing*, **46**(6):1558-1570. [doi:10.1109/78.678469]

Welcome visiting our journal website: <http://www.zju.edu.cn/jzus>

Welcome contributions & subscription from all over the world

The editor would welcome your view or comments on any item in the journal, or related matters

Please write to: Helen Zhang, Managing Editor of JZUS

E-mail: jzus@zju.edu.cn Tel/Fax: 86-571-87952276/87952331